Nanoscale Res Lett (2009) 4:873–877
DOI 10.1007/s11671-009-9329-3

NANO EXPRESS

Surface Localization of Buried III–V Semiconductor Nanostructures

P. Alonso-González · L. González · D. Fuster · J. Martín-Sánchez · Yolanda González

Received: 4 March 2009 / Accepted: 24 April 2009 / Published online: 9 May 2009

Abstract In this work, we study the top surface localization of InAs quantum dots once capped by a GaAs layer grown by molecular beam epitaxy. At the used growth conditions, the underneath nanostructures are revealed at the top surface as mounding features that match their density with independence of the cap layer thickness explored (from 25 to 100 nm). The correspondence between these mounds and the buried nanostructures is confirmed by posterior selective strain-driven formation of new nanostructures on top of them, when the distance between the buried and the superficial nanostructures is short enough ($d = 25$ nm).

Keywords Droplet epitaxy · III–V Semiconductor nanostructures · MBE

Introduction

The integration of semiconductor quantum dots (QD) as active elements in new quantum optoelectronic devices [1–4] requires a precise control in their shape, size and location over the substrate. In this direction, different strategies have been followed in the last years with promising results. One of them is the use of patterned substrates [5–9], in which good results on the growth selectivity and photoluminescence (PL) emission of single QD have been obtained [5–7]. Another approach based on droplet epitaxy growth technique [10, 11] has recently emerged as an optimal strategy for obtaining different nanostructures complexes [12, 13] with a great control in shape and size. Recently, our group has reported the ability to use this technique to obtain low density InAs QD with control in size into previously formed GaAs nanoholes [14]. In this previous work, we advanced the possibility of using certain capping growth conditions for marking the underneath nanostructures by the formation of mounding features at the top surface. The possibility of top surface localization of buried QD has been studied in the past by the growth of stacked structures [1] and more recently, by evaluating the surface morphology once a single layer of QD is capped [3]. As it is well known, the surface of a thin layer covering nanometric features is not flat, but it shows characteristic mounding features [3, 14–17]. However, when the thickness of the cap layer increases, these features enlarge and coalesce [15, 16] discarding any further correspondence of the mounds with the buried nanostructures. The possibility to overcome this problem is of high technological interest for the fabrication of devices, as single photon emitters, where the location of the nanostructures after being buried is a critical issue.

In this work, by means of preferential nucleation of InAs at the top surface, we demonstrate that mounds formed during the growth of the cap layer unequivocally mark the buried nanostructures. Additionally, we show that these surface features can be maintained up to 100-nm thick cap layers by the use of low temperature atomic layer molecular beam epitaxy (ALMBE) growth technique [18]. The different contributions to the surface chemical potential that influence on the selective preferential growth [19] are discussed in the framework of these results.

P. Alonso-González (✉) · L. González · D. Fuster · J. Martín-Sánchez · Y. González
Instituto de Microelectrónica de Madrid (IMM-CNM, CSIC), Isaac Newton, 8 Tres Cantos, Madrid 28760, Spain
e-mail: palonso@imm.cnm.csic.es

Experimental Procedure

The experimental procedure starts growing a 0.5-μm thick undoped GaAs(001) buffer layer by molecular beam epitaxy (MBE) at a growth rate $r_g = 0.5$ monolayers per second (ML/s), As_4 beam equivalent pressure (BEP) of 2×10^{-6} Torr and substrate temperature $T_s = 580$ °C on GaAs (001) substrates. The root mean square roughness of this surface is typically 0.24 nm. Then a nanotemplate fabrication process is performed by droplet epitaxy [11]. It consists of a two-step process where metallic Ga droplets are first formed on the surface to be finally exposed to an As atmosphere. In particular, the growth protocol followed for the formation of Ga droplets consists in the opening of the Ga shutter during 20 s, with the cell providing a flux equivalent to the growth of GaAs at 0.5 ML/s. Simultaneously, the As cell is pulsed in cycles of 0.2 s open/0.8 s close at a BEP(As_4) $= 5 \times 10^{-7}$ Torr. The result of this process is the formation of Ga droplets spread all over the surface with a density of 2×10^8 cm^{-2}. Finally, these Ga droplets are annealed under As atmosphere during 6 min at BEP(As_4) $= 5 \times 10^{-7}$ Torr [13]. During this annealing step, the In cell is also opened, depositing 1.4 ML of InAs, at $r_g = 0.01$ ML/s, for QD formation inside the nanoholes [14]. After this annealing and simultaneous InAs deposition step, the formed nanostructures are finally exposed during 1 min to As_2 flux at $T_s = 510$ °C and BEP(As_2) $= 3.5 \times 10^{-7}$ Torr.

The formed QD, with dimensions 14 ± 1 nm in height, 50 ± 2 nm in diameter and density 2×10^8 cm^{-2} (Fig. 1a), are then capped by a 50-nm thick GaAs layer. In particular, the first 15 nm of GaAs were grown at $T_s = 510$ °C and As_2 BEP changing from 5×10^{-7} to 9×10^{-7} Torr while the remaining 35 nm under typical MBE conditions: $T_s = 580$ °C and BEP(As_4) $= 2 \times 10-^6$ Torr. The surface that results after this process is shown in Fig. 1b. As expected, coalesced mounds elongated along the GaAs [1–10] direction are observed [15, 16]. In this sense, in order to study the resulting cap layer surface morphology and its possible correlation with the buried nanostructures, two different GaAs cap layers with thicknesses of 25 and 100 nm were grown. In the case of growing a 25-nm thick cap layer, the growth conditions followed were similar to that used in the case of growing the 50-nm thick cap layer; thus, the initial 15 nm were grown at $T_s = 510$ °C and As_2 BEP changing from 5×10^{-7} to 9×10^{-7} Torr while the remaining 10 nm of GaAs, under typical MBE conditions. As shown below (Fig. 2a), under this process, the cap layer shows a morphology consisting of a flat surface with isolated mounds. In the case of the 100-nm thick cap layer growth, the first 20 nm are initially grown as before, $T_s = 510$ °C and As_2 BEP changing from 5×10^{-7} to 9×10^{-7} Torr, and the remaining 80 nm are deposited at $T_s = 450$ °C and BEP(As_4) $= 2 \times 10-^6$ Torr using the ALMBE growth technique [18], with the aim of preserving as much as possible the mounding morphology achieved after the growth of the thinner cap layer ($d = 0\,25$ nm). After the growth of either 25- or 100-nm thick GaAs cap layers, different amounts of InAs were finally deposited to reveal the existence and hierarchy of sites for enhanced nucleation of new nanostructures. In particular 1.4, 1.5 and 1.6 ML of InAs were deposited at 0.01 ML/s, $T_s = 510$ °C and BEP(As_4) $= 5 \times 10^{-7}$ Torr. These samples were studied by atomic force microscopy (AFM).

In order to compare the optical quality of InAs QD after the different growth processes followed for the 25- and 100-nm thick cap layers, PL studies were performed after depositing 1.4 ML of InAs into the GaAs nanoholes. These PL measurements were carried out at 30 K, by using a standard setup with a frequency-doubled Nd:YAG laser ($\lambda_{exc} = 532$ nm) as excitation source, with a spot diameter of approximately 200 μm.

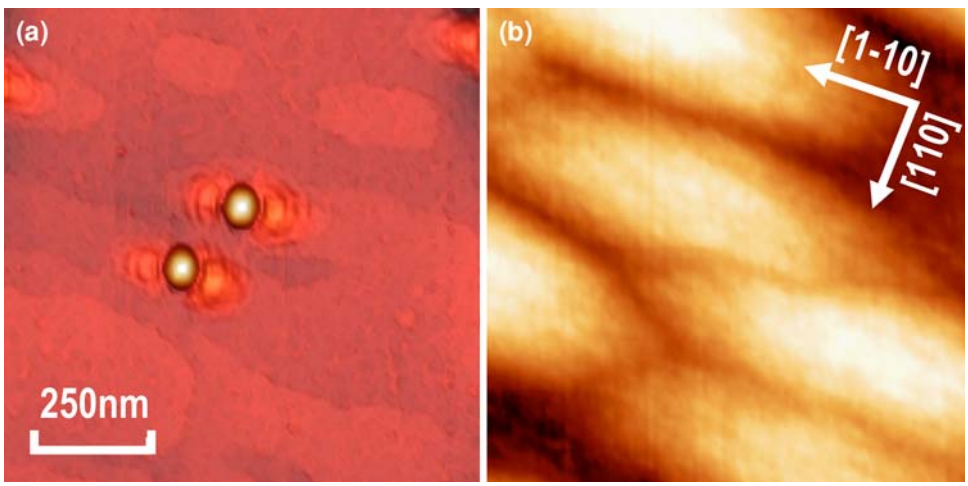

Fig. 1 1 μm × 1 μm AFM images corresponding to: **a** the initial InAs QD formed into GaAs nanoholes fabricated by droplet epitaxy and **b** the GaAs surface that results after capping by 50 nm of GaAs the nanostructures shown in (**a**) at typical MBE growth conditions. Coalesced mounds elongated along the [1–10] GaAs direction are observed

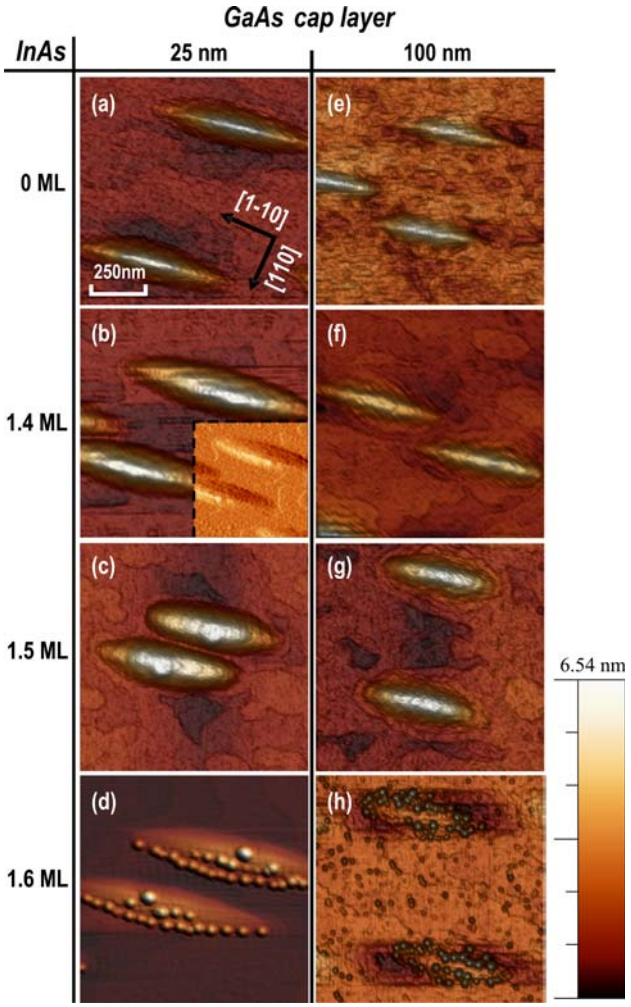

Fig. 2 Left column shows 1×1 μm^2 3D AFM images of the mounding surface that results after growing a 25-nm thick GaAs cap layer (**a**) and after 1.4 ML (**b**), 1.5 ML (**c**) and 1.6 ML (**d**) of InAs is deposited on this surface. The inset in (**b**) corresponds to the derivative image and is shown to highlight the presence of 3D InAs nuclei forming at the top of the mounds. Right column shows 1×1 μm^2 3D AFM images of the mounding surface that results after growing a 100-nm thick GaAs cap layer (**e**) and after 1.4 ML (**f**), 1.5 ML (**g**) and 1.6 ML (**h**) of InAs is deposited on this surface. See text for the growth conditions of the different GaAs cap layers

Results and Discussion

Figure 2 shows 1 μm × 1 μm 3D AFM images of capped InAs QD and posterior top surface InAs deposition. The corresponding images are distributed in columns for the two different cap layer thicknesses grown (25 and 100 nm) and in files for the different amount of InAs deposited (0, 1.4, 1.5 and 1.6 ML). It is first noticeable in this image that the surface morphology obtained just after capping the nanostructures is similar independently of the cap layer thickness (Fig. 2a, 2e). In particular, mounds elongated along the direction [1–10] are observed; their dimensions for the 25-nm thick cap layer samples are around 700 nm in length, 150 nm in width and 7 nm in height. It is also noticeable the coincidence between the density of the observed mounds and the nanostructures previously deposited (Fig. 1a). Thus, the most plausible is that below each mound, there is a QD.

Assuming that the mounds are located just over buried QD, new InAs material deposited on the surface would preferentially nucleate at their top if the underlying strain is large enough. In the case of 25-nm thick cap layers, Fig. 2b shows the AFM image after depositing 1.4 ML of InAs on the mounding surface shown in Fig. 2a. Notice that the amount of InAs deposited is far from the critical for QD formation on a flat surface under the used experimental conditions ($\sim$1.7 ML). This means that we would not expect QD formation unless InAs growth is enhanced at preferential sites of the surface. However, we observe incipient InAs clusters appearing on top of each mound (Fig. 2b). These InAs nanostructures are clearly observed in the derivative AFM image at the inset of this Fig. 2b. This result corroborates our initial supposition about the presence of a QD underneath each of the surface mounds. As expected, if more InAs is deposited, Fig. 2c, bigger nanostructures are formed on the top of these surface features. Figure 2d shows the situation when 1.6 ML of InAs is deposited on the surface. With this amount of InAs, besides the QD formed at the top of the mounds, we observe QD decorating the sidewalls of the mounds. This result indicates that once the QD at the top surface reaches an equilibrium size, the steps forming the mounds become new preferential nucleation sites for InAs material. This result means that, besides strain-related nucleation mechanisms, another energetic term that takes into account also curvature-related considerations in the selective nucleation of InAs material [19] has to be considered.

Similar to these experiments, Fig. 2e–g show the top surface morphology that results after capping the nanostructures with a 100-nm thick GaAs layer and posterior deposition of different amounts of InAs material. Comparing with the case of using a 25-nm thick cap layer (Fig. 2a–d), we find significant similarities in the mounding morphology and differences in the nucleation of InAs nanostructures at the top surface. First, as above commented, we observe mounds with the same density as that of the buried nanostructures and with similar dimensions, except for a lower height of 4 nm, than in the case of using 25-nm thick cap layers. This result means that the growth process used in this work for thick GaAs cap layers (100 nm) allows to maintain the morphology initially obtained for 25-nm thick cap layers. In this sense, the result shown in Fig. 2e is of great importance for most applications where thick cap layers and top surface localization are strictly necessary.

Respect to the deposition of InAs on this surface, 1.4, 1.5 and 1.6 ML in Fig. 2f–h, respectively, it is not observed in this case, any formation of InAs nanostructures at the top of the mounds. This result indicates that the non-uniform strain profile induced by the buried nanostructures does not propagate up to a distance of 100 nm, and therefore, only curvature-related effects have to be considered in the preferential nucleation of InAs. In a similar way to the previous result obtained for the thinner cap layer (25 nm, Fig. 2d), when the amount of InAs deposited is 1.6 ML (Fig. 2h), that is, when the critical thickness for the growth of QD on a flat surface is almost reached, well-defined QD at the sidewalls of the mounds are obtained together with the formation of incipient InAs islands all over the flat surface. It can be noticed that, as a difference to that observed in Fig. 2d, QD are now nucleated at both side walls of the mounds.

The results shown in Fig. 2 indicate a dependence of the formation of QD at the apex of the mounds with the strain profile induced from the buried nanostructures, which decreases with the GaAs cap layer thickness. The cap layer thickness seems to also be determinant in the nucleation of QD in the sidewalls of the mounds: Fig. 2d, h show that after depositing 1.6 ML of InAs, QD nucleate only on one of the side walls in the case of using 25-nm thick GaAs cap layers, while QD appear in both side walls of the mounds when a 100-nm thick GaAs cap layer is grown. This result could be understood on the basis of a different surface curvature (i.e. step density) and/or in the strain profile in the sidewalls of the mounds when cap layers of different thickness are grown.

Similar results corroborating a direct correspondence of the mounds formed at the top surface and the underneath nanostructures have been previously reported by our group for Ga(As)Sb Qrings formed on GaAs(001) substrates [20]. In that case, mounds with Qrings nucleated on top of them were observed once a 50-nm thick GaAs cap layer was grown over a first layer of nanostructures.

Finally, Fig. 3 shows the PL emission spectra from InAs QD capped by 25 nm (black line) and 100 nm (red line) thick GaAs layers. A slight increase of intensity is observed in the case of the 100-nm thick GaAs cap layer that could be ascribed to the larger distance from the QD to the air/GaAs interface [21]. The similar PL spectra observed in both samples indicates that the low substrate temperature process followed to keep the mounding morphology after growing thick cap layers has no influence on the optical properties of the InAs QD.

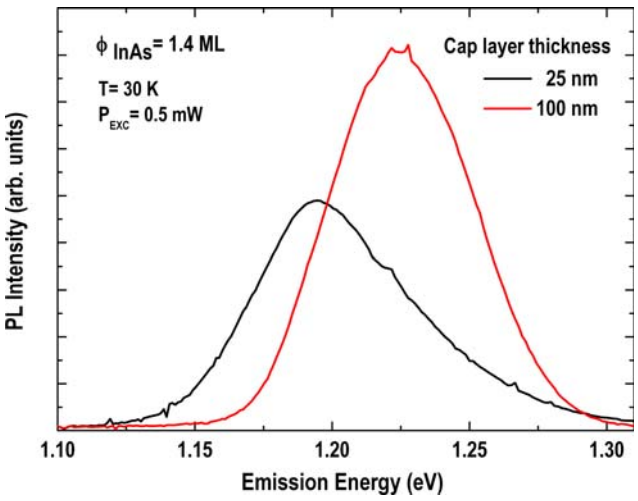

Fig. 3 Photoluminescence (PL) intensity spectra for 1.4 ML of InAs deposited into GaAs nanoholes capped by 25 nm (*black line*) or 100 nm (*red line*) thick GaAs layers

Conclusions

On balance, we have demonstrated that after an appropriate capping of InAs QD, the resulting GaAs top surface show a characteristic mounding morphology that permits a direct localization of buried nanostructures even at cap layer thickness as large as 100 nm. Different experiments, based on the nucleation of new nanostructures at the top surface of 25- and 100-nm thick GaAs cap layers, have permitted to establish a one-to-one correspondence between the mounds and the buried nanostructures. The results obtained also permit a direct observation of the different preferential sites for nanostructures formation driven by strain and/or curvature related mechanisms. The results presented in this work are of high-technological interest for the fabrication of those devices, as single photon emitters, where the nanostructures location after being buried is a critical issue.

Acknowledgements The authors gratefully acknowledge the financial support by the Spanish MICINN (TEC2008-06756-C03-01, Consolider-QOIT CSD2006-0019), CAM (S-505/ESP/000200) and by the European Commission through SANDIE Network of Excellence (No. NMP4-CT-2004-500101). P.A.G. thanks the I3P program.

References

1. A. Badolato, K. Hennessy, M. Atatüre, J. Dreiser, E. Hu, P.M. Petroff, A. Imamouglu, Science **308**, 1158 (2005). doi:10.1126/science.1109815
2. R.M. Stevenson, R.J. Young, P. Atkinson, K. Cooper, D.A. Ritchie, A.J. Shields, Nature **439**, 179 (2006). doi:10.1038/nature04446
3. K. Henessy, A. Badolato, M. Wigner, D. Gerace, M. Atatüre, S. Gulde, D. Fält, E.L. Hu, A. Imamoglu, Nature **445**, 896 (2007). doi:10.1038/nature05586
4. P.M. Intallura, M.B. Ward, O.Z. Karimov, Z.L. Yuan, P. See, A.J. Shields, P. Atkinson, D.A. Ritchie, Appl. Phys. Lett. **91**, 161103 (2007). doi:10.1063/1.2799756

5. H.Z. Song, T. Usuki, Y. Nakata, N. Yokoyama, H. Sasakura, S. Muto, Phys. Rev. B **73**, 115327 (2006). doi:10.1103/PhysRevB.73.115327
6. S. Kiravittaya, M. Benyoucef, R. Zapf-Gottwick, A. Rastelli, O.G. Schmidt, Appl. Phys. Lett. **89**, 233102 (2006). doi:10.1063/1.2399354
7. P. Atkinson, M.B. Ward, S.P. Bremner, D. Anderson, T. Farrow, G.A.C. Jones, A.J. Shields, D.A. Ritchie, Jpn J. Appl. Phys. **45**(Part 1), 2519 (2006). doi:10.1143/JJAP.45.2519
8. J. Martín-Sánchez, Y. González, L. González, M. Tello, R. García, D. Granados, J.M. García, F. Briones, J. Cryst. Growth **284**, 313 (2005). doi:10.1016/j.jcrysgro.2005.06.055
9. P. Alonso-González, L. González, Y. González, D. Fuster, I. Fernández-Martínez, J. Martín-Sánchez, L. Abelmann, Nanotechnology **18**, 355302 (2007). doi:10.1088/0957-4484/18/35/355302
10. T. Mano, K. Watanabe, S. Tsukamoto, H. Fujioka, M. Oshima, N. Koguchi, J. Cryst. Growth **209**, 504 (2000). doi:10.1016/S0022-0248(99)00606-5
11. Z.M. Wang, B.L. Liang, K.A. Sablon, G.J. Salamo, Appl. Phys. Lett. **90**, 113120 (2007). doi:10.1063/1.2713745
12. J.H. Lee, Z.M. Wang, N.W. Strom, Y.I. Mazur, G.J. Salamo, Appl. Phys. Lett. **89**, 202101 (2006). doi:10.1063/1.2388049
13. P. Alonso-González, B. Alén, D. Fuster, Y. González, L. González, J. Martínez-Pastor, Appl. Phys. Lett. **91**, 163104 (2007). doi:10.1063/1.2799736
14. P. Alonso-González, D. Fuster, L. González, J. Martín-Sánchez, Y. González, Appl. Phys. Lett. **93**, 183106 (2008). doi:10.1063/1.3021070
15. G. Constantini, A. Rastelli, C. Manzano, P. Acosta-Diaz, R. Songmuang, G. Katsaros, O.G. Schmidt, K. Kern, Phys. Rev. Lett. **96**, 226106 (2006). doi:10.1103/PhysRevLett.96.226106
16. A. Ballestad, B.J. Ruck, M. Adamcyk, T. Pinnington, T. Tiedje, Phys. Rev. Lett. **86**, 2377 (2001). doi:10.1103/PhysRevLett.86.2377
17. K.A. Sablon, Z.M. Wang, G.J. Salamo, L. Zhou, D.J. Smith, Nanoscale Res. Lett. **3**, 530 (2008). doi:10.1007/s11671-008-9194-5
18. F. Briones, L. González, A. Ruiz, Appl. Phys. A **49**, 729 (1989). doi:10.1007/BF00617001
19. B. Yang, F. Liu, M.G. Lagally, Phys. Rev. Lett. **92**, 025502 (2004). doi:10.1103/PhysRevLett.92.025502
20. P. Alonso-González, L. González, D. Fuster, Y. González, A.G. Taboada, J.M. Ripalda, A.M. Beltrán, D.L. Sales, T. Ben, S.I. Molina, Cryst. Growth Des. **9**(2), 1216 (2009). doi:10.1021/cg801186w
21. C.F. Wang, A. Badolato, I. Wilson-Rae, P.M. Petroff, E. Hu, J. Urayama, A. Imamoglu, Appl. Phys. Lett. **85**, 3423 (2004). doi:10.1063/1.1806251